Standing Friedel Waves: A Quantum Probe of Electronic States in Nanoscale Devices

Jun-Qiang Lu,[1] X.-G. Zhang,[1,2] and Sokrates T. Pantelides[3,4]

[1]*Center for Nanophase Materials Sciences, Oak Ridge National Laboratory, Oak Ridge, Tennessee 37831, USA*
[2]*Computer Science and Mathematics Division, Oak Ridge National Laboratory, Oak Ridge, Tennessee 37831, USA*
[3]*Materials Science and Technology Division, Oak Ridge National Laboratory, Oak Ridge, Tennessee 37831, USA*
[4]*Department of Physics and Astronomy, Vanderbilt University, Nashville, Tennessee 37235, USA*

(Received 11 June 2007; published 30 November 2007)

We report a theoretical study of the dynamic response of electrons in a metallic nanowire or a two-dimensional electron gas under a capacitively coupled "spot gate" driven by an ac voltage. A dynamic *standing Friedel wave* (SFW) is formed near the spot gate and near edges and boundaries, analogous to the static Friedel oscillations near defects. The SFW wavelength is controlled by the ac voltage frequency and the device's Fermi velocity, whereby the latter can be measured. In addition, the SFW amplitude exhibits resonant behavior at driving frequencies that are related to eigenenergy spacings in the device, allowing their direct measurement.

DOI: 10.1103/PhysRevLett.99.226804 PACS numbers: 73.20.Mf, 73.21.Hb, 73.50.Mx

The electron density around defects in a metal is known to exhibit "Friedel oscillations," produced by a singularity in the derivative of the dielectric function at the Fermi energy [1]. It is possible to obtain direct scanning-tunneling-microscopy (STM) images of Friedel oscillations produced by impurities and steps on metal surfaces [2,3] and even by impurities at semiconductor surfaces [4,5]. Giant Friedel oscillations were observed to arise from impurities and defects at the high-electron-density metallic surface layer of Be crystals [6]. Theoretical calculations predicted unique features for Friedel oscillations in 1D interacting electron systems [7].

In this Letter, we report simulations that demonstrate a dynamic analogue of the static Friedel oscillation in nanoscale 1D and 2D devices (Fig. 1). We use a "spot gate" capacitively coupled to a device, a setup that can be implemented with a sharp STM tip. The application of an ac voltage generates what we call a "standing Friedel wave" (SFW), a real wave with a frequency controlled by the gate signal. In contrast to the static Friedel oscillations, whose wavelength is π/k_F, where k_F is the Fermi wave vector, the wavelength of the SFW deviates from π/k_F by an amount that is proportional ω/v_F, where v_F is the Fermi velocity and ω is the driving frequency. Thus, by measuring the SFW wavelength, one effectively measures the device's Fermi velocity with directional resolution. The amplitude of the wave, also controlled by the gate signal, exhibits resonances when the driving frequency matches the spacing of the eigenenergies of the quantum states. These resonances can be used to probe the electronic states in nanoscale devices.

Before we expand on the new results, it is useful to contrast them with two other applications of ac voltages for the measurement of device properties. A capacitively coupled STM using an ac voltage has been used in the past to study nonlinear effects from higher harmonic response of the samples [8–10]. In the present case, such a setup can be used to generate SFWs both around the tip and at defects, but a second STM tip would be necessary to probe the SFW itself. The separation between the two tips can be on a macroscopic scale, as long as this distance is within the spatial range of the ac response of the sample. Separately, several authors studied theoretically the effect of an ac voltage on the source-drain current of devices, including tunnel junctions, contrasting the resulting ac current-voltage characteristics with the dc steady-state characteristics [11–16]. In the present case, we have no source-drain voltage or current, only an ac gate voltage at a sharp tip, which sets up SFWs that can be probed by a second STM tip.

We start by considering an infinite homogeneous (1D or 2D) system under an external field $V_{\text{ext}}(\mathbf{x}, t)$ applied using a "spot" gate, as depicted in Fig. 1. The spot gate is a gate electrode with a sufficiently small area [the region where $V_{\text{ext}}(\mathbf{x}, t) \neq 0$, e.g., the "area" of an STM tip] to produce large Fourier components $V_{\text{ext}}(\mathbf{q}, \omega)$ at finite $\mathbf{q}$. The charge-density response in this system is

$$\delta\rho(\mathbf{q}, \omega) = \chi(\mathbf{q}, \omega)V(\mathbf{q}, \omega) = \Theta(\mathbf{q}, \omega)V_{\text{ext}}(\mathbf{q}, \omega), \quad (1)$$

where $V = V_{\text{ext}} + V_{\text{ind}}$ is the sum of the external (V_{ext}) and the induced (V_{ind}) fields, and χ is the susceptibility. We define $\Theta(\mathbf{q}, \omega)$ to be the *charge response function* that will be the focus of this Letter. It is given by

$$\Theta(\mathbf{q}, \omega) = \frac{\chi(\mathbf{q}, \omega)}{\epsilon(\mathbf{q}, \omega)}, \quad (2)$$

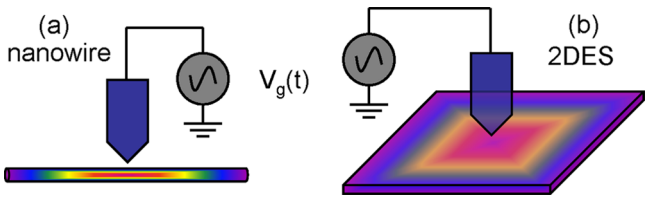

FIG. 1 (color online). Schematic sketch of the SFW setup: (a) a quasi-1D nanowire and (b) a 2DES.

where $\epsilon(\mathbf{q}, \omega)$ is the Lindhard dielectric function, which we write as $\epsilon(\mathbf{q}, \omega) = 1 - \chi(\mathbf{q}, \omega)/C(\mathbf{q})$. The quantity $[C(\mathbf{q})]^{-1}$ is the Fourier transform of the Coulomb potential. It has the familiar form $[C(\mathbf{q})]^{-1} = 1/\epsilon_0|\mathbf{q}|^2$ in three dimensions (3D), but takes more complicated forms in 1D [17] and 2D [18] (see below). The susceptibility is given by [19]

$$\chi(\mathbf{q}, \omega) = \frac{2e^2}{\Omega} \sum_{n\mathbf{k}} \frac{f(E_{n\mathbf{k}}) - f(E_{n\mathbf{k}-\mathbf{q}})}{E_{n\mathbf{k}} - E_{n\mathbf{k}-\mathbf{q}} - \hbar\omega + i\eta}, \quad (3)$$

where Ω is the volume, $E_{n\mathbf{k}}$ is the energy dispersion with the band label n, $f(E)$ is the Fermi-Dirac distribution function, and η is an infinitesimal smearing factor. The 1D or 2D systems can be realized, for example, in a metallic nanowire grown on a Si substrate and in a Si channel of a metal-oxide-semiconductor structure. In the latter case, contributions of the valence electrons to $\chi(\mathbf{q}, \omega)$ can be approximated through an overall scaling factor κ in $\epsilon(\mathbf{q}, \omega)$, and yield, $\epsilon(\mathbf{q}, \omega)/\kappa = 1 - \chi_c(\mathbf{q}, \omega)/C(\mathbf{q})$, where $\chi_c(\mathbf{q}, \omega)$ contains only the conduction band contribution from Eq. (3), and κ is the intrinsic dielectric constant of the nanodevice. If the device is metallic then $\chi_c(\mathbf{q}, \omega)$ contains all of the response and we can take $\kappa = 1$.

In 1D or 2D, the form of $C(\mathbf{q})$ differs from that in 3D because of two factors [17,18]: different dimensionality leads to different $\mathbf{q}$ dependence; furthermore, additional external screening by charges outside the device, e.g., in a dielectric substrate, changes $C(\mathbf{q})$ into $\kappa_b C(\mathbf{q})$, where κ_b is the dielectric constant of the substrate [17]. In this sense, the Fourier transform of $\kappa_b C(\mathbf{q})$ into real space can be viewed as the effective *capacitance density* of the device. Including κ_b, the dielectric function becomes

$$\frac{\epsilon(\mathbf{q}, \omega)}{\kappa} = 1 - \frac{\chi_c(\mathbf{q}, \omega)}{\kappa_b C(\mathbf{q})}. \quad (4)$$

The limit of complete external screening, namely $\kappa_b = \infty$, can be viewed as a noninteracting electron gas. This limit is unique to 1D and 2D systems for which an external polarizer can exist. In this limit, $\epsilon(\mathbf{q}, \omega) = \kappa$, but the charge response is still controlled by $\chi_c(\mathbf{q}, \omega)$ via Eq. (2), i.e., $\Theta(\mathbf{q}, \omega) = \chi_c(\mathbf{q}, \omega)/\kappa$. As expected, κ reduces the amplitude of the charge response.

The intrinsic dielectric constant κ and that of the substrate κ_b have opposite effects on the linear response from the conduction electrons. The former screens all fields, including the applied field, whereby it always reduces the effect of interest here. The latter screens only the induced field, whereby it serves to minimize the screening effect of the Coulomb interaction between the free charges in the device and enhances the effect of interest here. Below we will assume that $\kappa = 1$ which maximizes the effect, and we discuss the effect with different values of κ_b.

According to Eq. (2), the dynamic charge response produces resonant waves at wave vectors $\mathbf{q}$ for which $\epsilon(\mathbf{q}, \omega) = 0$ [20]. These are the conventional plasma waves. In addition, there are resonance waves due to the singularities of the susceptibility which are given by the poles of Eq. (3) at the Fermi energy, $E_{\mathbf{k}_F} = E_{\mathbf{k}_F-\mathbf{q}} - \hbar\omega$ (there may be multiple $\mathbf{k}_F$'s). These contain both the plasma and the Friedel waves. The solutions are

$$\mathbf{q} \cdot \mathbf{v}_F = \begin{cases} \pm\omega, & \text{plasma wave;} \\ 2\mathbf{k}_F \cdot \mathbf{v}_F \pm \omega, & \text{Friedel wave,} \end{cases} \quad (5)$$

where $\mathbf{v}_F = -\partial E_{\mathbf{k}}/\partial \mathbf{k}|_{E=E_F}$ is the Fermi velocity. The plasma waves in 1D and 2D do not have a constant frequency as in 3D, consistent with the previous 2D result [20]. The susceptibility is symmetric between $\mathbf{q}$ and $-\mathbf{q}$. If the exciting potential V_{ext} is also symmetric in $\mathbf{q}$ (i.e., its location does not move with time), then the charge response has equal amplitude for both $\mathbf{q}$ and $-\mathbf{q}$, resulting in a standing wave. That is what we call the SFW.

From Eq. (5), the singularities near $|\mathbf{q}| = 2k_F$ are split into pairs at finite frequencies, where $\Delta\mathbf{q} \cdot \mathbf{v}_F = 2\omega$. This small separation leads to a long-wavelength modulation of the SFW. If the modulation of the SFW can be generated and detected, it can be used to extract the Fermi velocity of the material. For smaller κ_b, the corresponding expressions that relate the wave vector shift to ω and $\mathbf{v}_F$ are somewhat more complicated, but the basic idea is the same.

The charge response for a 3D electron gas at zero frequency and at finite frequency for $\mathbf{q} \to \mathbf{0}$ are both well known. The latter yields the plasma resonance frequency. The Friedel oscillations, however, occur at a finite $|\mathbf{q}|$. For our purposes, we need the full charge response at both finite $\mathbf{q}$ and finite ω and for geometry other than a 3D bulk system. This function can be evaluated numerically for 1D and 2D systems. In Fig. 2 we plot the real part of the charge response function $\Theta(\mathbf{q}, \omega)$ of an infinite homogeneous nanowire at two frequencies $\omega = 0.23$ GHz and 0.23 THz, as a function of $\mathbf{q}$. We used the parameters derived from data in Ref. [21] for a GaAs nanowire: $k_F = 0.1\ \text{nm}^{-1}$, $E_F = 1.5$ meV, and $\kappa_b C = 8.3e/(\text{nm V})$. For comparison, we also show the results for infinite screening ($\kappa_b = \infty$). The imaginary part (the time dependence 90° out of phase) of $\Theta(\mathbf{q}, \omega)$ is not plotted. In Fig. 2(c) we show the temperature dependence of the resonance for the GaAs nanowire with $E_F = 1.5$ meV. Larger values of E_F would give sharper resonances at the same temperature.

Unlike the static Friedel oscillations, a SFW can be generated in an infinite defect-free wire using a sufficiently sharp gate electrode whose spatial dimension is smaller than the Fermi wavelength. In Fig. 3 we show the SFW at two different frequencies in an infinite homogeneous GaAs nanowire under an ac perturbation from a very sharp spot gate electrode placed at $x = 0$. The applied field is assumed to be $V_{\text{ext}}(x, t) = V_0 e^{-x^2/d^2} e^{-i\omega t}$, with a strength $V_0 = 0.1$ V and a width $d = 10$ nm. At the higher frequency, the modulation of the SFW is clearly evident. The modulation has a wave vector $\Delta q = 2\omega/|\mathbf{v}_F|$ in agreement with Eq. (5). The long-wavelength wave with twice the period of the modulation corresponds to the plasma reso-

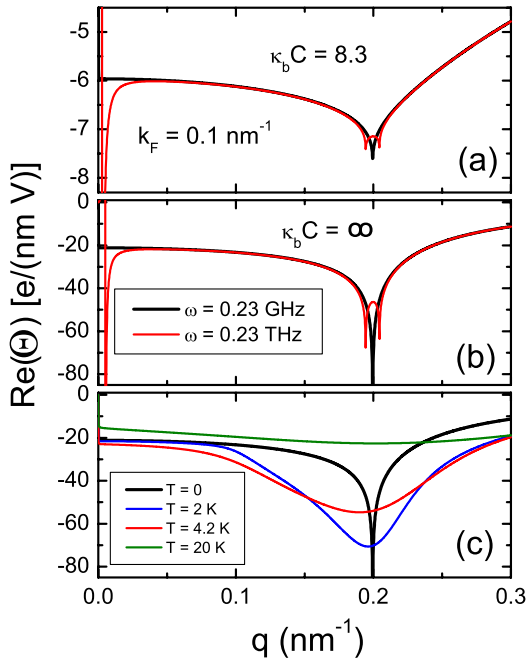

FIG. 2 (color online). Charge response function $\Theta(\mathbf{q}, \omega)$ of an infinite homogeneous nanowire at two different frequencies: (a) with $\kappa_b C = 8.3e/(\mathrm{nm\,V})$, (b) with $\kappa_b \to \infty$, and (c) for $\omega = 0.23$ GHz at different temperatures.

nance. The imaginary part of the charge response is proportional to the frequency and becomes significant at $\omega = 0.23$ THz.

Similar to the static Friedel oscillations, the SFW can also be observed near the boundaries of a finite system. For a finite system, it is convenient to calculate the dielectric function in real space. The usual expression for the susceptibility in terms of the eigenenergies E_l can be rewritten in terms of Green's functions,

$$\chi(\omega;\mathbf{r},\mathbf{r}') = \frac{e^2}{i\pi}\int dE\{[f(E)-f(E_-)]G^R(E_-;\mathbf{r},\mathbf{r}') \times G^A(E;\mathbf{r}',\mathbf{r}) + f(E)[G^A(E;\mathbf{r},\mathbf{r}') \times G^A(E_+;\mathbf{r}',\mathbf{r}) - G^R(E_-;\mathbf{r},\mathbf{r}')G^R(E;\mathbf{r}',\mathbf{r})]\}, \tag{6}$$

where G^A and G^R are the advanced and the retarded Green functions, respectively, and $E_\pm = E \pm \hbar\omega$.

If we discretize real space into a finite number of mesh points, then the applied field $V_{\mathrm{ext}}(\mathbf{r})$ and the charge response $\delta\rho(\mathbf{r})$ are both vectors, and the Lindhard function $\chi(\omega;\mathbf{r},\mathbf{r}')$ and the effective capacitance density $C(\mathbf{r},\mathbf{r}')$ are both matrices. The effective capacitance matrix is defined by $\mathbf{V}_{\mathrm{ind}}(\omega) = \mathbf{C}^{-1}\delta\rho(\omega)$, which is the discretized version of the Coulomb potential and leads to the linear-response equation,

$$\delta\rho(\omega) = \mathbf{C}[\mathbf{C} - \chi(\omega)]^{-1}\chi(\omega)\mathbf{V}_{\mathrm{ext}}(\omega). \tag{7}$$

Equations (6) and (7) give the dynamic charge response.

The SFWs produced in finite-size nanowire and 2DES are shown in Fig. 4. In this figure we use the materials parameter as the GaAs nanowire and a broader gate with a width $d = 2\pi/|\mathbf{k}_F|$. The length of the nanowire is 1570 nm. The gate voltage has a width $d = 62.8$ nm with strength $V_0 = 0.1$ V. In Fig. 4(b) the size of the rectangular-shaped 2DES is 490 nm × 245 nm. The applied field is $V_{\mathrm{ext}}(\mathbf{r},t) = V_0 e^{-|\mathbf{r}|^2/d^2} e^{-i\omega t}$, with $d = 62.8$ nm and $V_0 = 0.1$ V. A parametrized tight-binding Hamiltonian is used to compute the Green's functions in Eq. (6). For the nanowire, the Hamiltonian is $H = \epsilon\sum_i c_i^\dagger c_i + t\sum_i c_i^\dagger c_{i+1}$, with $\epsilon = 0$ and $t = \hbar^2/2ma^2$,

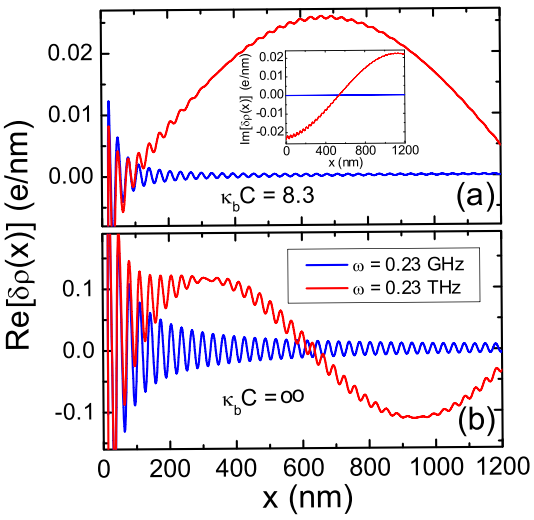

FIG. 3 (color online). Standing Friedel wave in an infinite homogeneous nanowire generated by a sharp spot gate: (a) with $\kappa_b C = 8.3e/(\mathrm{nm\,V})$ (inset shows the imaginary part) and (b) with $\kappa_b \to \infty$.

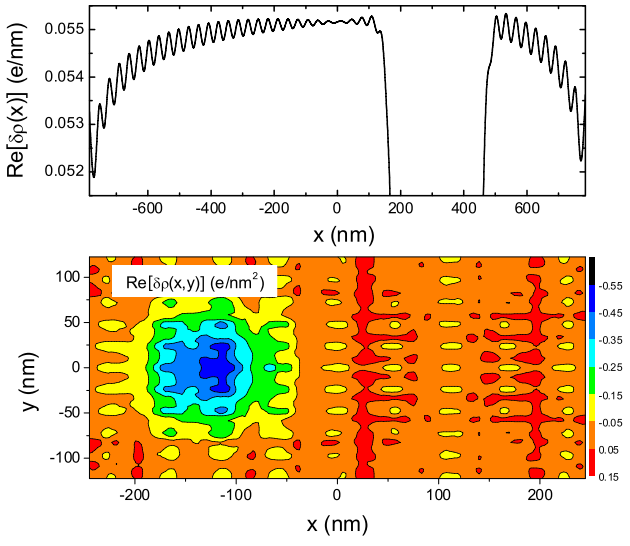

FIG. 4 (color online). Standing Friedel wave in (a) a nanowire with a finite length and (b) a 2DES with a rectangular geometry. Both calculations use the substrate screening $\kappa_b C = 8.3e/(\mathrm{nm\,V})$.

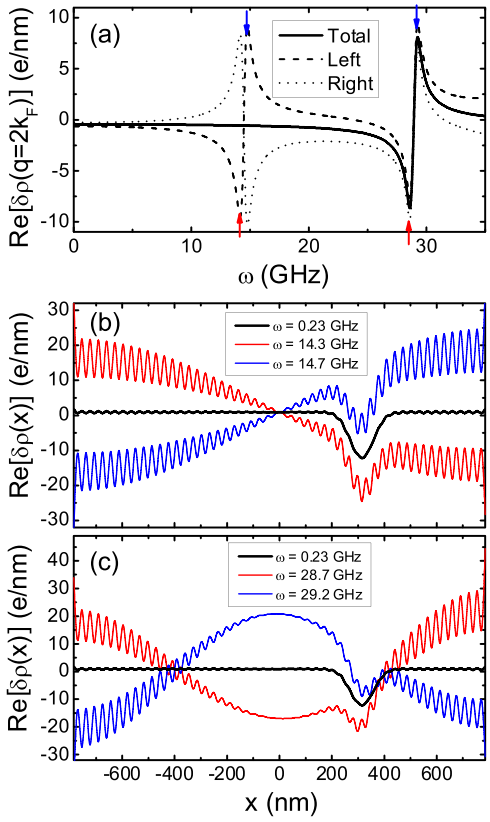

FIG. 5 (color online). Resonances in a nanowire with $\kappa_b \to \infty$: (a) Fourier transform of $\delta\rho$ in the frequency domain at $q = 2k_F$; (b), (c) spatial distributions of $\delta\rho$ just below (red curves) and above (blue curves) the resonances. The two resonances in (a) are at $\omega = 14.5$ GHz and $\omega = 28.9$ GHz, and the arrows indicate the frequencies for the curves in (b) and (c).

where $a = 15.7$ nm is the spacing between the mesh points. For the 2DES, a square lattice is chosen, using the nearest neighbor coupling $t = \hbar^2/2ma^2$ where $a = 8$ nm.

The frequency dependence of the SFW shows a series of resonances as depicted in Fig. 5, where the Fourier transforms of the charge response $\delta\rho(x)$ for a GaAs nanowire are plotted. Here to highlight the resonances we use a strong substrate screening $\kappa_b \to \infty$. Coulomb interaction will shift and reduce the resonances moderately and will superimpose a strong plasma wave. For a 1D system, the resonances are alternately odd (the oscillation on the left half of the nanowire is opposite in sign than that on the right) and even in parity, determined by the parity of $l - l'$, where l and l' label the eigenenergies E_l. Figure 5(b) shows the real-space charge oscillation at an odd-parity resonance, and 5(c) shows an even-parity resonance. Despite the asymmetric excitation and response, the Fourier components of the odd resonances are exactly zero if one integrates over the entire nanowire [the solid curve labeled "total" in Fig. 5(a)]. Therefore, we also plot the Fourier transforms using only the left or right halves of the nanowire, shown as the dashed curves labeled "left" and "right," respectively. These resonances arise from the singularities in the susceptibility whenever $\hbar\omega = E_l - E_{l'}$ for any pair of l and l' with $E_l < E_F$ and $E_{l'} > E_F$. They can be a powerful probe of the electron eigenstates in a nanodevice.

In conclusion, we propose that nanoscale devices exhibit a dynamic response to an external ac field analogous to the static Friedel oscillation that originates from defects. The dynamic response, SFW, can be used to probe quantum mechanical and electronic properties of nanoscale devices, such as the directionally resolved Fermi velocity and the energy differences of quantum-well levels. Semiconductor heterostructures may provide the best platform to observe this effect.

This research was conducted at the CNMS sponsored at ORNL by the Division of Scientific User Facilities, US DOE. The work was further supported by the DOE Grant No. FDEFG0203ER46096, by NSF Grant No. ECS-0524655, and by the McMinn Endowment at Vanderbilt University.

[1] J. Friedel, Nuovo Cimento Suppl. **7**, 287 (1958).
[2] M. Xu, Z. Xiao, K. Sagisaka, M. Kitahara, and D. Fujita, Nanotechnology **15**, S341 (2004).
[3] Y. Hasegawa and Ph. Avouris, Phys. Rev. Lett. **71**, 1071 (1993).
[4] M. C. M. M. van der Wielen, A. J. A. van Roij, and H. van Kempen, Phys. Rev. Lett. **76**, 1075 (1996).
[5] K. Kanisawa, M. J. Butcher, H. Yamaguchi, and Y. Hirayama, Phys. Rev. Lett. **86**, 3384 (2001).
[6] P. T. Sprunger, L. Petersen, E. W. Plummer, E. Legsgaard, and F. Besenbacher, Science **275**, 1764 (1997).
[7] R. Egger and H. Grabert, Phys. Rev. Lett. **75**, 3505 (1995).
[8] G. P. Kochanski, Phys. Rev. Lett. **62**, 2285 (1989).
[9] S. J. Stranick and P. S. Weiss, J. Phys. Chem. **98**, 1762 (1994).
[10] S. H. Tessmer, G. Finkelstein, P. I. Glicofridis, and R. C. Ashoori, Phys. Rev. B **66**, 125308 (2002).
[11] M. Buttiker, A. Pretre, and H. Thomas, Phys. Rev. Lett. **70**, 4114 (1993).
[12] N. S. Wingreen, A.-P. Jauho, and Y. Meir, Phys. Rev. B **48**, 8487 (1993).
[13] A. Pretre, H. Thomas, and M. Buttiker, Phys. Rev. B **54**, 8130 (1996).
[14] B. Wang, J. Wang, and H. Guo, Phys. Rev. Lett. **82**, 398 (1999).
[15] J. H. Oh, D. Ahn, and S. W. Hwang, Phys. Rev. B **71**, 205321 (2005).
[16] J. Maciejko, J. Wang, and H. Guo, Phys. Rev. B **74**, 085324 (2006).
[17] J. Lee and H. N. Spector, J. Appl. Phys. **57**, 366 (1985).
[18] J. Lee and H. N. Spector, J. Appl. Phys. **54**, 6989 (1983), The factor $1/\kappa$ in Eq. (4) was dropped in this reference but was included in Ref. [17].
[19] H. Ehrenreich and M. H. Cohen, Phys. Rev. **115**, 786 (1959).
[20] F. Stern, Phys. Rev. Lett. **18**, 546 (1967).
[21] E. Levy *et al.*, Phys. Rev. Lett. **97**, 196802 (2006).